Published in final edited form as:
Environ Sci Technol. 2018 May 15; 52(10): 5821–5829. doi:10.1021/acs.est.8b00224.

Measurements of Parameters Controlling the Emissions of Organophosphate Flame Retardants in Indoor Environments

Yirui Liang[†], **Xiaoyu Liu**[*,‡], and **Matthew R. Allen**[§]

[†]Oak Ridge Institute for Science and Education participant at U.S. Environmental Protection Agency, 1299 Bethel Valley Road, Oak Ridge, TN 37830, United States

[‡]Office of Research and Development, National Risk Management Research Laboratory, U.S. Environmental Protection Agency, Research Triangle Park, North Carolina 27711, United States

[§]Jacobs Technology, Inc. 600 William Northern Boulevard, Tullahoma, Tennessee 37388, United States

Abstract

Emission of semivolatile organic compounds (SVOCs) from source materials usually occurs very slowly in indoor environments due to their low volatility. When the SVOC emission process is controlled by external mass transfer, the gasphase concentration in equilibrium with the material (y_0) is used as a key parameter to simplify the source models that are based on solid-phase diffusion. A material-air-material (M-A-M) configured microchamber method was developed to rapidly measure y_0 for a polyisocyanurate rigid foam material containing organophosphate flame retardants (OPRFs). The emission test was conducted in 44 mL microchambers for target OPFRs, including tris(2-chloroethyl) phosphate (CASRN: 115–96-8), tris(1-chloro-2-propyl) phosphate (CASRN: 13674–84-5), and tris(1,3-dichloro-2-propyl) phosphate (CASRN: 13674–87-8). In addition to the microchamber emission test, two other types of tests were conducted to determine y_0 for the same foam material: OPFR diffusive tube sampling tests from the OPFR source foam using stainless-steel thermal desorption tubes and sorption tests of OPFR on an OPFR-free foam in a 53 L small chamber. Comparison of parameters obtained from the three methods suggests that the discrepancy could be caused by a combination of theoretical, experimental, and computational differences. Based on the y_0 measurements, a linear relationship between the ratio of y_0 to saturated vapor pressure concentration and material-phase mass fractions has been found for phthalates and OPFRs.

Graphical abstract

Corresponding Author:[*]Phone: 1-919-541-2459; Fax: 1-919-541-0359; liu.xiaoyu@epa.gov.

The authors declare no competing financial interest.

ASSOCIATED CONTENT

Supporting Information

The Supporting Information is available free of charge on the ACS Publications website at DOI: 10.1021/acs.est.8b00224.

The M-A-M microchamber; diffusive tube sampling test and materials for small chamber sorption test on storage rail; measured OPFR concentrations; details of analytical methods, experimental conditions, and model inputs; calculated Bi_m/K_{ma} and F_{om} values of SVOCs for different materials; and data of the relationship between y_0/V_p and mass fraction in materials for SVOCs (PDF)

The views expressed in this article are those of the authors and do not necessarily represent the views or policies of the U.S. EPA. Mention of trade names or commercial products does not constitute endorsement or recommendation for use by the U.S. EPA.

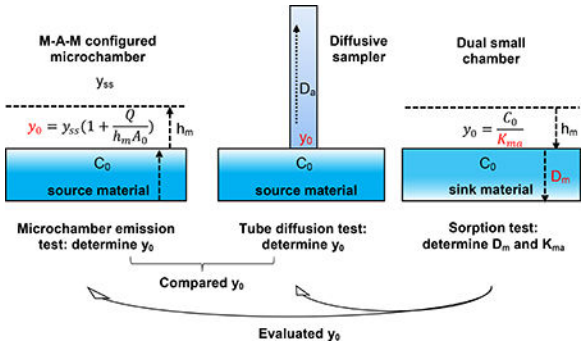

INTRODUCTION

Semivolatile organic compounds (SVOCs) are chemicals with vapor pressures ranging from 10^{-14} to 10^{-4} atm (10^{-9} to 10 Pa) at 25 °C. SVOCs can be found across a range of chemical classes and chemical functional uses, including phthalate esters, flame retardants, pesticides, and preservatives.[1] Among the SVOCs, organophosphate flame retardants (OPFRs) have been produced globally in large quantities and used extensively in a wide array of commercial products, such as polyvinyl chloride (PVC) floor coverings, furnishings, textile coatings, plastics, and electronic products.[2–5] Because OPFRs are not chemically bonded to product materials, slow emission of OPFRs from sources to the environment usually occurs.[6] Human exposure to OPFRs can occur through inhalation of indoor air and suspended particles, dermal absorption, and direct ingestion.[6–8] Adverse health effects associated with humans and animals, including damage to the reproductive system, carcinogenicity, endocrine disruption, and adverse neurodevelopmental effects, have been found for OPFRs such as tris(2-chloroethyl) phosphate (TCEP), tris(1-chloro-2-propyl) phosphate (TCPP), and tris(1,3-dichloro-2-propyl) phosphate (TDCPP).[6] As a result, the fate and transport of OPFRs and human exposure to these pollutants have emerged as a high priority research topic over the years.

Researchers have studied the mass transfer mechanisms for SVOCs for years to understand the fate and transport of these compounds in indoor environments.[9] Xu and Little developed a mass transfer model for SVOC emissions and identified that the emissions of SVOCs are controlled by parameters that include the initial material-phase concentration of the SVOC (C_0, $\mu g/m^3$), the material-phase diffusion coefficient (D_m, m^2/h), the material/air partition coefficient (K_{ma}, dimensionless), and mass transfer coefficients across the source and sorption surfaces (h_m and h_s, m/h). Later, Xu et al. found that for SVOCs with very low volatility, such as di-2ethylhexyl phthalate (DEHP), diffusion within the source material can be ignored, and the gas-phase concentration in equilibrium with the material (y_0) is a key parameter controlling the emissions of SVOCs. Notably, three assumptions must be made to use y_0 as the key parameter for a source material. First, both D_m and K_{ma} are independent of the concentration. Second, the off-gassing of the SVOCs is controlled by the external mass transfer across the material surface, and diffusion within the material is negligible. Third, y_0 remains constant throughout the emission process, which is valid with large partitioning coefficients (e.g., $K_{ma} > 10^8$) and large initial concentrations (e.g., $C_0 > 10\%$ by weight). With respect to only the emission process, whether the internal material diffusion is

negligible is dependent on the Fourier number for mass transfer ($Fo_{m,}$ dimensionless) and the ratio of the Biot number for mass transfer (Bi_m, dimensionless) to K_{ma}:

$$Fo_m = \frac{D_m t}{L^2} \quad (1)$$

$$\frac{Bi_m}{K_{ma}} = \frac{h_m L}{D_m K_{ma}} \quad (2)$$

where t (h) is the time, and L (m) is the thickness of the source material. The dimensionless number Bi_m/K_{ma} represents the ratio of internal mass transfer resistance (material diffusion) to the external mass transfer resistance (mass transfer across the material surface). Fo_m represents the ratio of a compound's diffusion rate to its storage rate in the substrate. For instance, if Bi_m/K_{ma} is greater than 35 when Fo_m equals 10^{-4}, internal diffusion controls the emissions of the compounds, and external mass transfer is negligible. Essentially, the primary goal of the published studies on the characterization of SVOC diffusion was to determine these key parameters. Considerable efforts have thus been made to estimate these model parameters.

Early chamber studies on SVOC emissions were conducted using standard chambers, including the Chamber for Laboratory Investigation of Materials, Pollution, and Air Quality (CLIMPAQ) and the Field and Laboratory Emission Cell (FLEC),[–] designed for measuring the emissions of volatile organic compounds (VOCs). These studies revealed the substantial difficulties associated with chamber tests for SVOCs of very low volatility. For instance, due to the strong sink effect, it may take up to years for SVOCs to reach steady state, and surface adsorption is hard to avoid through the sampling pathways. Xu et al. designed a special chamber with a high ratio of emission area to adsorption area and successfully measured the emission of DEHP from vinyl flooring within a month. Inspired by this chamber design, Liang and Xu explicitly measured the values of y_0 and the stainless steel surface/air partition coefficient for multiple phthalates with a multi-inlet-and-outlet improved chamber, which further reduced the test period for phthalates to less than a week, with the measured values of y_0 ranging from 0.02 to 24.7 $\mu g/m^3$ for various vinyl flooring at 25 °C. The specially designed chambers significantly improved the measurements of SVOC emissions over traditional chambers (FLEC and CLIMPAQ); however, this design relies on the flexibility and imperviousness of the material to form an airtight cavity, which limits its viability for materials that are pervious. Therefore, improvements are still needed to apply the specially designed chamber to various other types of materials.

Cao et al. developed an innovative C_m-history method to simultaneously measure y_0 and the cloth/air partition coefficient for several phthalates. Later, they measured y_0 for DEHP emitted form PVC flooring using the solid-phase microextraction (SPME) method. Recently, Wu et al. proposed a diffusion-based passive sampling method using standard stainless-steel thermal desorption tubes to measure y_0 and the stainless steel tube surface/air partition

coefficient for phthalates. Wu et al. further extended their diffusion-based method to measuring the value of the surface/air partition coefficient independently for different impervious indoor surfaces and found that surface roughness plays an important role in the adsorption process. In contrast to previous chamber studies,[9] the SPME method and the diffusion-based tube method[10] are much simpler because these methods do not involve any ventilated space and thus avoid considering mass transfer across surfaces. Although these sealed chamber/tube methods are highly innovative and effective in determining y_0 for source materials, some concerns arise regarding the uncertainty of these methods. First and foremost, these methods were developed based on the constant y_0 assumption and may not be applicable when Bi_m/K_{ma} is greater than 1 (both internal and external mass transfer need to be considered). An experiment conducted by Ni et al. indicated that the y_0 of TCPP for wallpaper samples decreased significantly over the test period of 280 days. In a more recent study, Pei et al. observed a similar decrease trend of y_0 through a 60-day emission test of TCPP from flexible polyurethane foam. Second, these methods were only applied to determine y_0 for materials containing phthalates; therefore, their viability remains unknown for other SVOCs. Third, the distance from the sampling device to the test material is important for mathematical calculations and yet remained unclear in the methods cited. Moreover, all of the methods assumed a linear equilibrium surface/air relationship, which may not be true as demonstrated in experimental studies and the mathematical model. Last, these methods have not included porous materials for which the gas diffusion into the material needs to be considered. Because of these reasons, there is a need to justify these methods for SVOCs other than phthalates and to develop more convenient means to estimate y_0 values for materials. For estimating D_m and K_{ma} in sink materials, Liu et al.[11] developed a method based on a degree of sorption saturation (DSS) model and characterized the sorption properties of polychlorinated biphenyl (PCB) congeners and OPFRs. The sorption test method is applicable to various materials, including those with permeable surfaces.

In this study, three types of tests (microchamber emission test, diffusive tube sampling test, and dual small chamber sorption test) have been applied to determine the emission parameters for OPFRs. The specific objectives are to (1) develop an improved material-air-material (M-A-M) configured microchamber that is self-sealed to rapidly measure the value of y_0 for polyisocyanurate rigid (PIR) foam containing OPFRs, (2) apply the diffusive tube sampling test method and the dual small chamber sorption test method to determine y_0 for the PIR foam and compare with the y_0 values obtained from the microchamber emission test, (3) propose a simple and rapid method to estimate y_0 values for source materials of SVOCs, and (4) compare the advantages and disadvantages of different SVOC testing methods for future research.

METHODS AND MATERIALS

Chemicals.

Certified TCEP, TCPP, and TDCPP calibration standards were purchased from AccuStandard, Inc. (New Haven, CT, USA). An isotopically labeled compound, tributyl phosphate-D_{27} (99.5% purity, Cambridge Isotope Laboratories, Inc., Andover, MA, USA), was used as the internal standard on the gas chromatography/mass spectrometry (GC/MS)

system. Triphenyl phosphate-D_{15} (98% purity, Sigma-Aldrich, St. Louis, MO, USA) was used as the extraction recovery check standard (RCS). Chromatography-grade methylene chloride (Burdick and Jackson, Muskegon, MI, USA) and ethyl acetate (OmniSoly, Billerica, MA, USA) were used as solvents in the extraction and cleaning without further purification. The solvents were regularly analyzed to monitor potential contamination with OPFRs.

Materials.

PIR foam material made by ICL-IP America, Inc. (Gallipolis Ferry, WV, USA) was used as the OPFR emission source material. The TCEP, TCPP, and TDCPP contents in the foam material were 2, 4, and 14% by weight, respectively. The same type of PIR foam material, which was also made by ICL-IP America. Inc. but free of OPFRs, was used as the sorption material to measure D_m and K_{ma} for TCEP, TCPP, and TDCPP. The thickness of both types of PIR foam materials was approximately 4 mm. Prior to the tests, the foam materials were wrapped in aluminum foil and stored at room temperature.

M-A-M Configured Microchamber Emission Test.

The microchamber (Markes International, Llantrisant, U.K.) consisted of an open-ended cylinder (cup) constructed of Silicosteel-coated stainless steel with a depth of 25 mm, a diameter of 45 mm, and a volume of 44 mL that was reconfigured as a M-A-M emission chamber. As shown in Figure S1, two pieces of foam materials were placed at the bottom and top of the microchamber using double sided tapes (the tape was extracted prior to the test, and no OPFRs were found within the material). Because the microchamber was selfsealed, it did not require the materials to be impervious. Two microchambers with identical OPFR PIR foam placed inside were connected in series and ventilated with dry clean air. The flow rate through each microchamber was maintained at approximately 200 mL/min, resulting in an air change rate of 273 h^{-1}. Measurements were conducted at a temperature of 23 ± 1 °C. The microchambers were ventilated with clean air for 600 h during the tests. Polyurethane foam (PUF) (small precleaned certified, Supelco, St. Louis, MO, USA) samples were collected at the faceplate of the chamber to monitor the gas-phase concentrations of emitted OPFRs.

Diffusive Tube Sampling Test.

Stainless steel thermal desorption tubes (89 mm length, 5 mm ID, 6.3 mm OD, Markes International, Llantrisant, U.K.) were used as the diffusive samplers. Each tube was prepacked with 200 mg of Tenax TA by the manufacturer. The diffusion system includes two stainless steel cylinders, one standard thermal desorption tube, and one stainless steel shim. The larger cylinder (5 cm OD × 5 cm L) is designed to hold the tube in a direction perpendicular to the test material. To prevent direct contact, a shim (0.127 ± 0.013 mm thickness, 5.23 mm ID, 7.87 mm OD, Model Number 91182A401, McMaster, Elmhurst, IL, USA) was placed between the Tenax tube and test material. The smaller stainless steel cylinder (2.5 cm OD × 5 cm length) served as a cap to push the sorbent tube and shim against the material surface. The diffusive tube sampling test setup is presented in Figure S2a). Tenax tubes containing accumulated OPFRs were collected at different time periods

(i.e., 2, 4, 8, 16, 24 h, etc.) during the test. More details of the diffusive sampler and diffusive tube sampling procedure can be found in Wu et al.'s article.

Dual Small Chamber Sorption Test.

The test was conducted using two 53 L electropolished stainless steel chambers, one as the source chamber and the other as the material test chamber. Both chambers were connected in series in a temperature-controlled incubator (Model SCN4−52, Environmental Equipment Co., Inc., Cincinnati, OH, USA). The chamber design and construction followed the ASTM Standard Guide D5116–10. A 5 cm diameter computer cooling fan (Model EC4020, Evercool Thermal Corp., Ltd., Taiwan) was installed in each chamber to provide air mixing in the chamber space. Measurements were conducted at 23 ± 1 °C, 50% relative humidity, and 1 h^{-1} air change rate. NonOPFR PIR foam was cut into cylinder buttons (average diameter was 1.26 cm). The buttons were then mounted on aluminum scanning electron microscope specimen pin mounts (Ted Pella, Inc., Redding, CA, USA) with double-sided tape and were secured on rails whose surfaces were saturated with gas-phase OPFRs prior to the test (Figure S2b). PUF samples were collected to determine the chamber air concentration, and button samples were collected to measure sorption of OPFR on the materials during the test. More details of chamber setting and test procedure can be found in previous studies.[9]

Sample Extraction and Analysis.

After PUF sample collection, each PUF cartridge was capped in a glass holder, wrapped in aluminum foil, placed in a sealable plastic bag, and refrigerated at 4 °C until analysis. PUF samples were placed in individual 40 mL borosilicate glass amber I-Chem vials (Thermo Scientific, Waltham, MA, USA) with approximately 35 mL 1:1 methylene chloride/ethyl acetate ($MeCl_2$/EtOAC) and 25 μL of 20 μg/mL RCS and extracted horizontally on the Multipurpose Lab Rotator (Barnstead International Model 2346, Thermo Scientific, Waltham, MA, USA) for 1 h. The extract was filtered through anhydrous sodium sulfate and further concentrated to approximately 1.5 mL using the RapidVap N_2 Evaporation System (Model 791000, LabConco, Kansas City, MO, USA). The PIR foam and material buttons removed from the dual small chamber sorption test were extracted using a sonicator (Ultrasonic Cleaner FS30, Fisher Scientific, Pittsburgh, PA, USA) with 10 mL of 1:1 methylene chloride/ethyl acetate (Fisher Scientific, Pittsburgh, PA, USA) and 50 μL of 20 μg/mL recovery check standard for 30 min in a scintillation vial. The concentrated extract was then transferred to a 5 mL volumetric flask and brought up to volume with rinse solution from the concentration tube for GC/MS (Agilent 6890A/5973N GC/MS) liquid analysis following the method described by Liu et al. The Tenax tube samples collected in the diffusive tube sampling test were analyzed on a thermal desorber (Markes TD100) and Agilent 6890A/5973N GC/MS system. Detailed information on instrumental parameters is provided in Tables S1 and S2, and the instrument calibration ranges are listed in Table S3.

Determination of y_0 from M-A-M Microchamber Emission Test.

In the microchamber, assuming that a boundary layer exists above the chamber surfaces, and that the internal material diffusion is negligible, the accumulation of gas-phase SVOC in the chamber obeys the following mass balance:

$$V\frac{dy}{dt} = Q(y_{in} - y) + h_m A_0(y_0 - y) - h_s A_s(y - y_s) \quad (3)$$

where V (m^3) is the chamber volume, Q (m^3/h) is the ventilation rate through the microchamber, y ($\mu g/m^3$) is the gas-phase SVOC concentration in the chamber, y_{in} ($\mu g/m^3$) is the inlet gas-phase SVOC concentration, A_0 (m^2) is the total emission area of the top and bottom foam in the chamber, h_s (m/h) is the mass transfer coefficient across the side wall surface of the microchamber, A_s (m^2) is the area of the side wall surface of the microchamber, and y_s ($\mu g/m^3$) is the gas-phase SVOC concentration in the boundary layer adjacent to the side wall surface of the microchamber in the test. The chamber wall surface-phase SVOC concentration can be calculated by

$$K_{sa}\frac{dy_s}{dt} = h_s(y - y_s) \quad (4)$$

where K_{sa} (m) is the chamber wall surface/air partition coefficient. At steady state, dy/dt equals zero, assuming y_s equals y in eq 3, y_0 can be calculated by

$$y_0 = y_{ss}\left(1 + \frac{Q}{h_m A_0}\right) \quad (5)$$

where y_{ss} ($\mu g/m^3$) is the steady state gas-phase SVOC concentration in the chamber, which can be directly measured using PUF during tests. The value of y_0 can be determined directly from eq 5, where value of h_m can be estimated by empirical equations based on the average air velocity.

Determination of y_0 from Diffusive Tube Sampling Test.

The SVOC diffusion model developed by Wu et al. was applied in this study. In this method, gas-phase SVOCs emitted from the source material diffuse into the air in the cylindrical space of a Tenax tube. As the SVOC diffuses through the air, adsorption will occur on the inner surface of the Tenax tube. The governing equation for the two-dimensional diffusion process using cylindrical coordinates (r,z) is

$$\frac{\partial C(r,z,t)}{\partial t} = \frac{1}{r}\frac{\partial}{\partial r}\left(rD_a\frac{\partial C(r,z,t)}{\partial r}\right) + D_a\frac{\partial^2 C(r,z,t)}{\partial z^2} \quad (6)$$

with the following boundary conditions:

- $C|_{surf} = y_0$ (at the surface of emission source, z = 0);
- $C|_{surf} = 0$ (at Tenax tube surface, z = L);

- $D_a \frac{\partial C}{\partial r}|_{surf} = K_{sa} \frac{\partial C}{\partial r}|_{surf}$ (at Tenax tube surface).

Where C (μg/m^3) is the gas-phase SVOC concentration in the Tenax tube, r is the tube radius, z is the height of the cylindrical space of the Tenax tube, D_a (m^2/h) is the diffusivity of the SVOC in air, and K_{sa} (m) is the Tenax tube inner surface/air partition coefficient. A complete derivation of this method is detailed in eqs 2–12 in Wu et al.'s article. The values of D_a for different SVOCs can be estimated using SPARC online calculator as in Wu et al.'s article or based on empirical correlations as in this study. With the measurement of the SVOC mass sorption in Tenax tubes at different time durations, the values of y_0 and K_{sa} can be determined by nonlinear regression. The mathematical solutions were obtained numerically using MATLAB (Mathworks, Inc. Natick, MA) in this study.

Determination of y_0 from Dual Small Chamber Sorption Test.

When the emission process is controlled by the external mass transfer, under the equilibrium condition, y_0 is assumed to be

$$y_0 = \frac{C_0}{K_{ma}} \quad (7)$$

Therefore, y_0 can be determined by measuring C_0 and K_{ma} of the source material. C_0 can easily be determined through material extraction measurement. In this study, we followed the method developed by Liu et al.' to determine K_{ma}. In addition, the material-phase diffusion coefficient (D_m) can be determined simultaneously. The two parameters were estimated by fitting the DSS model to experimentally measured sorption concentrations. The DSS model is defined as

$$\mathrm{DSS} = \frac{M(t)}{M_{max}} = \frac{M(t)}{C_a K_{ma} A \delta} = f\left(N_1, \mathbf{\Theta}, Fo_m\right) \quad (8)$$

$$M(t) = M_{max} \times DSS = f\left(K_{ma}, D_m, C_a, A, \delta, V, N, t\right) \quad (9)$$

where $M(t)$ (μg) is the amount of SVOC that has entered the sink material at time t, M_{max} (μg) is the maximum amount of the SVOC the sink material can absorb at a given air concentration, C_a (μg/m^3) is SVOC concentration in the air, A (m^2) is the exposed surface area of the sink material, δ (m) is the thickness of the sink material, N_1 is the dimensionless air change rate, Θ is the dimensionless mass capacity, N (h^{-1}) is the air change rate, D_m (m^2/h) is the material-phase diffusion coefficient for the chemical, and t (h) is time. In this method, TCEP, TCPP, and TDCPP belong to the same chemical class, in which the material/air partition coefficients are related to the vapor pressure (eq 9 by Liu et al.), and the material-phase diffusion coefficients are related to molecular weight (eq 10 by Liu et al.). A more detailed description of the DSS model is presented in Liu et al.'s study In this study,

the nonlinear regression fitting was performed using MATLAB to estimate the diffusion and partition coefficients from the experimental data for TCEP, TCPP, and TDCPP. The model fitting was applied simultaneously to the data sets for the three compounds to reduce the number of parameters to be estimated from a single data set.

Quality Assurance and Control

A quality assurance project plan (QAPP) was prepared and approved prior to measurements. The GC/MS calibration was verified by the internal audit program. Each batch of samples was analyzed along with its corresponding quality control samples. The extraction method blank and field blank samples were prepared and analyzed as well. All PUF and material samples were extracted and analyzed with the criteria that the percentage recovery of the recovery check standards had to be within 100 ± 25%, and that the precision of the duplicate samples had to be within ±25%. When the measured concentrations of OPFRs in the PUF sample were above the highest calibration level, the extract was diluted and reanalyzed. All Tenax tube samples were analyzed with the criteria that the precision of the duplicate samples had to be within ±25%.

RESULTS AND DISCUSSION

Measurements of OPFRs in PIR Foam.

The content of OPFRs in the foam materials was extracted and measured following the previously described sample extraction and analysis procedure. Measurement results of C_0 are listed in Table S4.

M-A-M Microchamber Emission Test.

As shown in Figures 1a and S3, gas-phase concentrations of TCEP and TCPP reached a steady state very rapidly during the microchamber test. Gas-phase TDCPP concentrations that were measured were below the quantification range and therefore are not reported. The average concentrations of TCEP and TCPP in microchamber 1 after reaching a steady state were 5.02 ± 0.54 $\mu g/m^3$ and 2.02 ± 0.27 $\mu g/m^3$ (n = 25), respectively (microchamber 2 data is presented in Table S4). The values of y_0 for TCEP and TCPP in the source material were calculated by eq 5, and mass transfer coefficients across source material surfaces were determined based on the air velocity measured above the surfaces. With knowing K_{sa} for TCEP and TCPP from a previous study, we further predicted the gas-phase concentrations in the microchamber following eqs 3 and 4, and the modeling results agreed reasonably well (correlation coefficient (R^2) > 0.75) with the measured concentrations (Figures 1a and S3). Input parameters for modeling the microchamber emission tests are listed in Table S4.

A limitation of the specially designed chamber is that the testing material needs to be flat, flexible, and impervious to be properly installed in the chamber. The M-A-M configured microchamber inherits the advantage of having a large emission surface to adsorptive surface area ratio (1.80) compared to other traditional chamber tests, as in the specially designed chamber, and features a self-sealed compartment, which does not require the emission material to be flat, flexible, or impervious. Eq 5 indicates that the attainment of a steady state is necessary for obtaining y_0, and the uncertainty of the calculation is related to

the mass transfer coefficient across the emission surface, h_m (y_{ss}, Q, and A_0 can be measured directly during the test). Although Liang and Xu experimentally determined h_m for their chamber design using dimethyl phthalate (DMP) as a reference chemical, the method is complicated and difficult to apply to other chambers and chemicals. The difficulty of obtaining accurate h_m reveals the limitation of the chamber tests for y_0 measurements. In this study, we explicitly measured the average air velocity in the chamber to represent the air velocities adjacent to the material surfaces and wall surfaces to estimate the mass transfer coefficient. This estimation method is based on empirical equations, and its accuracy is greatly dependent on the measurement of air velocity across the material surface and/or the chamber wall surface. In addition, h_m directly influences how fast gas-phase OPFR concentrations reach a steady state in the microchamber. It is noticeable in Figure 1a that the measured TCEP concentration reached a steady state faster than the modeling results. One possible reason is that h_m may be underestimated using the empirical method. Therefore, more accurate means for determining h_m values are needed for future SVOC research.

Diffusive Tube Sampling Test.

As a comparison, we also determined y_0 values of TCEP, TCPP, and TDCPP for the identical source material using the diffusive tube sampling test method. The test was conducted simultaneously at three different positions of the source material strip (Figure S2a). Therefore, three sets of data were obtained from the test (Figures 1b and S4). Using the method described by Wu et al., we fit the measured mass accumulation by diffusion at different time durations to determine y_0 and the Tenax tube surface/air partition coefficient (K_{sa}) simultaneously. The average R^2 values of the fitting for TCEP, TCPP, and TDCPP are 0.96, 0.91, and 0.91, respectively. Figure 1b shows that the measured mass of TDCPP was the highest among the three compounds in the diffusion test. One of the limitations of the diffusion test is the starting value issue associated with the nonlinear regression when fitting two parameters simultaneously. Compared with the microchamber emission test, which uses the same concept of y_0 as the diffusive tube sampling test, the y_0 values obtained from the latter are lower by 48–54% (Table 1). Other potential causes of the uncertainties of this method include (1) ignoring the solidphase diffusion process within the source material in the method; (2) assuming a linear adsorption isotherm between the concentration in the gas-phase and on the tube surface; (3) estimating the method of D_a; and (4) the lack of airtightness of the tested PIF foam compared to the PVC flooring tested by Wu et al. Further research is needed to assess the contribution of each factor to the overall uncertainties of this method.

Dual Small Chamber Sorption Test.

The mass accumulation of OPFRs in OPFR-free PIR foam over time is shown in Figure 1c. Using the DSS model, we fit the sorption data sets for TCEP, TCPP, and TDCPP simultaneously to obtain the values of D_m and K_{ma} in the material (Table 1). The application of the DSS method provided good fitting results ($R^2 > 0.9$). The values of D_m and K_{ma} estimated in this study are of the same order of magnitude as the previous estimates. The DSS model improves the starting value issue associated with nonlinear regression by linking a class of compounds (TCEP, TCPP, and TDCPP in this study) with their vapor pressures and molecular weights. Because of these constraints, the TCEP fitting result is slightly

below the measurement results (Figure 1c). Fitting each set of data may provide better fitting results but will also sacrifice the advantage of the DSS model in improving the nonlinear regression. It is notable, however, that this method does not fundamentally solve the issue. Liu et al. provided a detailed discussion on this issue with the DSS model. The parameters used for estimating D_m and K_{ma} in the DSS model are listed in Table S4.

As mentioned previously, the PIR foam material used in the dual small chamber sorption test is identical with the PIR foam material used in the microchamber emission test and the diffusive tube sampling test, the only difference being that the former does not contain any OPFRs. It is likely that D_m and K_{ma} for OPFRs are dependent on the level of C_0. However, given that the OPFRs are additives in the PIR foam, their influence on the physical and chemical properties of the tested PIR foam is limited. Moreover, K_{ma} can be considered constant if C_0 remains effectively constant. Therefore, we assumed that the values of both D_m and K_{ma} are independent of C_0 in this dual chamber sorption test method. Following eq 7, we calculated the value of y_0 for the PIR foam (Table 1). The calculated y_0 values by K_{ma} from the dual small chamber sorption test are over an order of magnitude higher than the values obtained from microchamber emission test or the diffusive sampling test for TCEP and TCPP. However, the difference between the y_0 value calculated by K_{ma} and the value obtained through the diffusion test for TDCPP is considerably smaller (less than four times). The dual chamber sorption method avoids the y_0 concept. Instead, it directly measures D_m and K_{ma} from sorption experiments. Its advantages and disadvantages have been discussed in the literature.[9] The y_0 in this method was simply calculated by eq 7, which is a rough estimate for a comparison purpose with the assumption that the emission process is controlled by external mass transfer. The discrepancy of y_0 values from these different methods could be caused by a combination of theoretical, experimental, and computational differences as discussed in this article. As mentioned previously, y_0 remains constant throughout the emission process if the material/air partitioning coefficient is large (e.g., $K_{ma} > 10^8$), and the initial concentration is at a high level (e.g., $C_0 > 10\%$ by weight). Among the three compounds, only TDCPP meets these requirements ($K_{ma} = 1.90 \times 10^8$ and $C_0 \sim 14\%$) of using a constant y_0 throughout the emission process. Following eq 1, the calculated values of Bi_m/K_{ma} for the PIR foam material are 3.43, 8.78, and 1.77, for TCEP, TCPP, and TDCPP, respectively (Table S5). The results indicate that the emission of TCEP and TCPP from the PIR foam material is possibly controlled by both internal and external mass transfer, which is also consistent with the observations in the literature.[9] However, D_m and K_{ma} were estimated simultaneously based on the DSS method, which assumes an infinite mass transfer coefficient above the sink materials, and thus the calculated Bi_m/K_{ma} as well as Fo_m values may not be very accurate. Therefore, there is an urgent need to develop an experimental method to determine D_m and K_{ma} independently with reduced uncertainty and improved accuracy. As a reference, we listed the calculation results of Fo_m and Bi_m/K_{ma} in Table S5 for SVOCs with available literature data in various indoor materials to determine whether internal (Bi_m/K_{ma} is much larger than 1), external (Bi_m/K_{ma} is close to or smaller than 1), or both mechanisms need to be considered.

Relationship between y_0, V_p, and Material Mass Fractions.

It is unfortunate that current experimental approaches[9] all involve model fitting to determine y_0 for SVOC source materials, including the microchamber emission test in this study. A more convenient means is needed to rapidly estimate y_0 values for target compounds. Although previous studies found that the value of y_0 for a vinyl flooring material is close to the saturated vapor pressure concentration ($V_{p,}$ $\mu g/m^3$) of DEHP at different temperatures, Little et al. suggested that y_0 cannot be well approximated by its corresponding V_p in all cases. Indeed, Liang and Xu explicitly showed that y_0 values of phthalates are lower than their vapor pressures, with a trend of a higher material phase concentration (C_0) corresponding to a higher y_0 value. A question whether the value of y_0 can be estimated based on C_0 and V_p has been raised. Cao et al. performed a nonlinear curve fit on y_0 values and mass fractions of DEHP in previous studies and found that there is an exponential relationship between y_0/V_p and mass fraction. Although the equation proposed by Cao et al. is very useful, its applicability for chemicals other than DEHP remains unknown. Using the available phthalate data from emission and diffusive tube sampling tests from the literature and OPFR data from this study, we examined the relationship between the ratio of y_0/V_p and the mass fraction in the source materials for various materials. For consistency, the OPFR data used in this analysis were obtained from the microchamber emission test and the diffusive sampling test in this study. Interestingly, we found that the ratio of y_0/V_p is linearly related to the mass fraction at low levels (<15%) in the source material at room temperature (23–25 °C) (Figure 2):

$$\frac{y_0}{V_p} = 3.40 \cdot \text{mass fraction} \quad (10)$$

The linear relationship we obtained is in a good agreement with the very recent finding of Eichler et al. on the equilibrium between the gas and material phase of phthalates and phthalate alternatives in PVC products. The inclusion of TCEP and TCPP in eq 10 extended the linear relationship from phthalates to other SVOCs. Although the acquired linear equation enables researchers to estimate y_0 without conducting complex experiments, the equation has some limitations, and cautions should be taken when using this equation. First and foremost, the SVOC vapor pressure is not always available, especially for SVOCs with very low volatility, which limits the application of eq 10. Second, the equation was obtained from the measurement results for phthalates and OPFRs (TCEP and TCPP), and its application to other types of SVOCs needs further investigation. Third, the y_0 values and vapor pressures involved in this analysis were measured at 25 °C (for TCEP and TCPP, y_0 values were measured at 23 °C, and their vapor pressures were obtained from the European Union Risk Assessment Report), so the relationship may not be viable under other temperatures. Last, due to the availability of y_0 values in the literature, the linear regression does not include SVOCs with high mass fractions (>15%). Further research is needed to validate if the linear relationship can be applied to source materials with high SVOC mass fractions. The values of y_0, V_p, and mass fractions in this analysis are listed in Table S6.

Experimental Measurements of y_0 for SVOC Source Materials.

To date, the y_0 values are mostly reported for phthalates, and this is the first systematic study measuring y_0 and other key parameters for other SVOCs using various methods. The test methods involved in this study (emission test, diffusive tube sampling test, and dual small chamber sorption test) generally represent current experimental approaches for measuring key parameters that control the emissions of SVOCs. The results in this study suggested that both ventilated chamber methods, such as the specially designed SVOC chambers, and the microchamber (this study), and diffusion-based sealed chamber methods, such as diffusive sampler and SPME-based sampler, can only be used to determine y_0 values for SVOC materials if the internal mass transfer within the material can be ignored. Therefore, knowledge of D_m and K_{ma} is necessary to judge whether the emission process can be simplified to use y_0 as a constant controlling parameter. Although the diffusion-based sealed chamber methods are generally novel and less time-consuming, their advantages over the ventilated chamber methods are not categorical. For example, all of the current sealed chamber methods are diffusion-based and assume a linear surface/air partition relationship. These methods, therefore, are not applicable to scenarios that involve a nonlinear surface/air partition relationship (e.g., Freundlich isotherm). Moreover, because the mathematical relationship between the measured mass accumulation (eq 6) and y_0 value is much more complicated than the mathematical relationship used for the ventilated chamber methods, the accuracy of the model fitting in diffusion-based tests needs additional analysis. Some diffusion-related parameters, e.g., diffusion length, also need further investigation for optimization purposes.

Supplementary Material

Refer to Web version on PubMed Central for supplementary material.

ACKNOWLEDGMENTS

We thank Mr. Ryan Daly from U.S. EPA for helping to operate the TD-GC/MS system, Dr. John Little's group at Virginia Tech for providing the diffusive tube sampling test apparatus, ICL Industrial Products America, Inc. for providing the PIR foam, and a former employee of U.S. EPA, Dr. Zhishi Guo, for his insightful comments.

REFERENCES

(1). Weschler CJ; Nazaroff WW Semivolatile organic compounds in indoor environments. Atmos. Environ 2008, 42, 9018–9040.

(2). Weschler CJ Changes in indoor pollutants since the 1950s. Atmos. Environ 2009, 43, 153–169.

(3). Van der Veen I; De Boer J Phosphorus flame retardants: properties, production, environmental occurrence, toxicity and analysis. Chemosphere 2012, 88, 1119–1153. [PubMed: 22537891]

(4). Wei G; Li D; Zhuo M; Liao Y; Xie Z; Guo T; Li J; Zhang S; Liang Z Organophosphorus flame retardants and plasticizers: sources, occurrence, toxicity and human exposure. Environ. Pollut 2015, 196, 29–46. [PubMed: 25290907]

(5). Wensing M; Uhde E; Salthammer T Plastics additives in the indoor environment- flame retardants and plasticizers. Sci. Total Environ 2005, 339, 19–40. [PubMed: 15740755]

(6). Stapleton HM; Klosterhaus S; Eagle S; Fuh J; Meeker JD; Blum A; Webster TF Detection of organophosphate flame retardants in furniture foam and U.S. house dust. Environ. Sci. Technol. 2009, 43, 7490–5. [PubMed: 19848166]

(7). Hartmann PC; Bü D; Giger W. Organophosphate flame retardants and plasticizers in indoor air. Chemosphere 2004, 57, 781–787. [PubMed: 15488569]

(8). U.S. Department of Health and Human Services, Agency for Toxic Substances and Disease Registry, Toxicology profile for phosphate ester flame retardants, September 2012, http://www.atsdr.cdc.gov/toxprofiles/tp.asp?id=1119&tid=239 (accessed April 17, 2018).

(9). Weschler CJ; Nazaroff WW SVOC exposure indoors: fresh look at dermal pathways. Indoor Air 2012, 22, 356–77. [PubMed: 22313149]

(10). Little JC; Weschler CJ; Nazaroff WW; Liu Z; Cohen Hubal EA Rapid methods to estimate potential exposure to semivolatile organic compounds in the indoor environment. Environ. Sci. Technol 2012, 46, 11171–8. [PubMed: 22856628]

(11). Stapleton HM; Klosterhaus S; Keller A; Ferguson PL; van Bergen S; Cooper E; Webster TF; Blum A Identification of flame retardants in polyurethane foam collected from baby products. Environ. Sci. Technol 2011, 45, 5323–5331. [PubMed: 21591615]

(12). Bradman A; Castorina R; Gaspar F; Nishioka M; Colon M; Weathers W; Egeghy PP; Maddalena R; Williams J; Jenkins PL; McKone TE. Flame retardant exposures in California early childhood education environments. Chemosphere 2014, 116, 61–66. [PubMed: 24835158]

(13). Liu X; Allen MR; Roache NF Characterization of organophosphorus flame retardants' sorption on building materials and consumer products. Atmos. Environ 2016, 140, 333–341.

(14). Liu Z; Ye W; Little JC Predicting emissions of volatile and semivolatile organic compounds from building materials: A review. Build. Environ 2013, 64, 7–25.

(15). Guo Z A framework for modelling non-steady-state concentrations of semivolatile organic compounds indoors – II. Interactions with particulate matter. Indoor Built Environ. 2014, 23, 26–43.

(16). Xu Y; Little JC Predicting emissions of SVOCs from polymeric materials and their interaction with airborne particles. Environ. Sci. Technol 2006, 40, 456–461. [PubMed: 16468389]

(17). Xu Y; Liu Z; Park J; Clausen PA; Benning JL; Little JC Measuring and predicting the emission rate of phthalate plasticizer from vinyl flooring in a specially-designed chamber. Environ. Sci. Technol 2012, 46, 12534–12541. [PubMed: 23095118]

(18). Guo Z Improve our understanding of semivolatile organic compounds in buildings. Indoor Built Environ. 2014, 23, 769–773.

(19). Zhang Y; Xiong J; Mo J; Gong M; Cao J Understanding and controlling airborne organic compounds in the indoor environment: mass transfer analysis and applications. Indoor Air 2016, 26, 39–60. [PubMed: 25740682]

(20). Xu Y; Zhang Y An improved mass transfer based model for analyzing VOC emissions from building materials. Atmos. Environ 2003, 37, 2497–2505.

(21). Clausen PA; Hansen V; Gunnarsen L; Afshari A; Wolkoff P Emission of di-2-ethylhexyl phthalate from PVC flooring into air and uptake in dust: emission and sorption experiments in FLEC and CLIMPAQ. Environ. Sci. Technol 2004, 38, 2531–2537. [PubMed: 15180047]

(22). Clausen PA; Liu Z; Xu Y; Kofoed-Sørensen V; Little JC Influence of air flow rate on emission of DEHP from vinyl flooring in the emission cell FLEC: Measurements and CFD simulation. Atmos. Environ 2010, 44, 2760–2766.

(23). Clausen PA; Liu Z; Kofoed-Sørensen V; Little J; Wolkoff P Influence of temperature on the emission of di-(2-ethylhexyl) phthalate (DEHP) from PVC flooring in the emission cell FLEC. Environ. Sci. Technol 2012, 46, 909–915. [PubMed: 22191658]

(24). Schossler P; Schripp T; Salthammer T; Bahadir M Beyond phthalates: Gas phase concentrations and modeled gas/particle distribution of modern plasticizers. Sci. Total Environ 2011, 409, 4031–4038. [PubMed: 21764421]

(25). Afshari A; Gunnarsen L; Clausen PA; Hansen V Emission of phthalates from PVC and other materials. Indoor Air 2004, 14, 120–8. [PubMed: 15009418]

(26). Liang Y; Xu Y Improved method for measuring and characterizing phthalate emissions from building materials and its application to exposure assessment. Environ. Sci. Technol 2014, 48, 4475–4484. [PubMed: 24654650]

(27). Cao J; Weschler CJ; Luo J; Zhang Y Cm-history method, a novel approach to simultaneously measure source and sink parameters important for estimating indoor exposures to phthalates. Environ. Sci. Technol 2016, 50, 825–834. [PubMed: 26677723]

(28). Cao J; Zhang X; Little JC; Zhang Y A SPME-based method for rapidly and accurately measuring the characteristic parameter for DEHP emitted from PVC floorings. Indoor Air 2017, 27, 417–426. [PubMed: 27238276]

(29). Wu Y; Xie M; Cox SS; Marr LC; Little JC A simple method to measure the gas-phase SVOC concentration adjacent to a material surface. Indoor Air 2016, 26, 903–912. [PubMed: 26609785]

(30). Wu Y; Eichler CMA; Leng W; Cox SS; Marr LC; Little JC Adsorption of phthalates on impervious indoor surfaces. Environ. Sci. Technol 2017, 51, 2907–2913. [PubMed: 28140579]

(31). Ni Y; Kumagai K; Yanagisawa Y Measuring emissions of organophosphate flame retardants using a passive flux sampler. Atmos. Environ 2007, 41, 3235–3240.

(32). Pei J; Yin Y; Cao J; Sun Y; Liu J; Zhang Y Time dependence of characteristic parameter for semi-volatile organic compounds (SVOCs) emitted from indoor materials. Build. Environ 2017, 125, 339–347.

(33). Liu X; Guo Z; Roache NF Experimental method development for estimating solid-phase diffusion coefficients and material/air partition coefficients of SVOCs. Atmos. Environ 2014, 89, 76–84.

(34). ASTM D5116–10 Standard guide for small-scale environmental chamber determinations of organic emissions from indoor materials/ products; ASTM International: West Conshohocken, PA, 2010.

(35). Guo Z Program PARAMS Users Guide; U.S. Environmental Protection Agency: Washington, DC, 2005.

(36). Liang Y; Liu X; Allen MR Measuring and modeling surface sorption dynamics of organophosphate flame retardants in chambers. Chemosphere 2018, 193, 754–762. [PubMed: 29175403]

(37). European Union Risk Assessment Report - TDCP CAS 13674− 87–8, May 2008 Tris [2-Chloro-1-(Chloromethyl) Ethyl] Phosphate (TDCP). https://echa.europa.eu/documents/10162/13630/trd_rar_ireland_tdcp_en.pdf (accessed April 17, 2018).

(38). Eichler CMA; Wu Y; Cao J; Shi S; Little JC Equilibrium relationship between SVOCs in PVC products and the air in contact with the product. Environ. Sci. Technol 2018, 52, 2918–2925. [PubMed: 29420885]

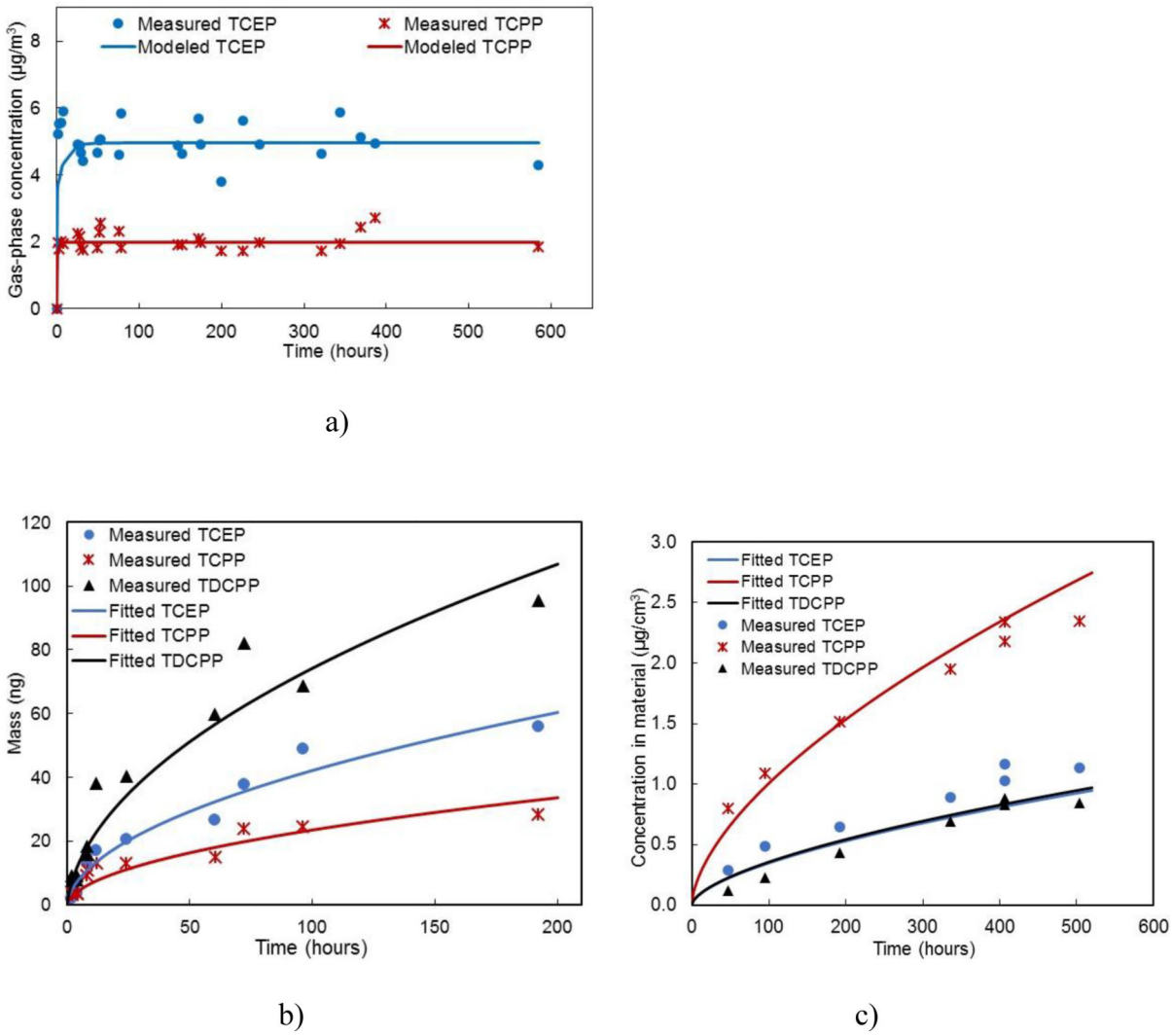

Figure 1.

Measured OPFR concentrations with model fittings (a) in the M-A-M Microchamber 1, (b) in a diffusive sampling test at Position 1, and (c) in the dual small chamber sorption test.

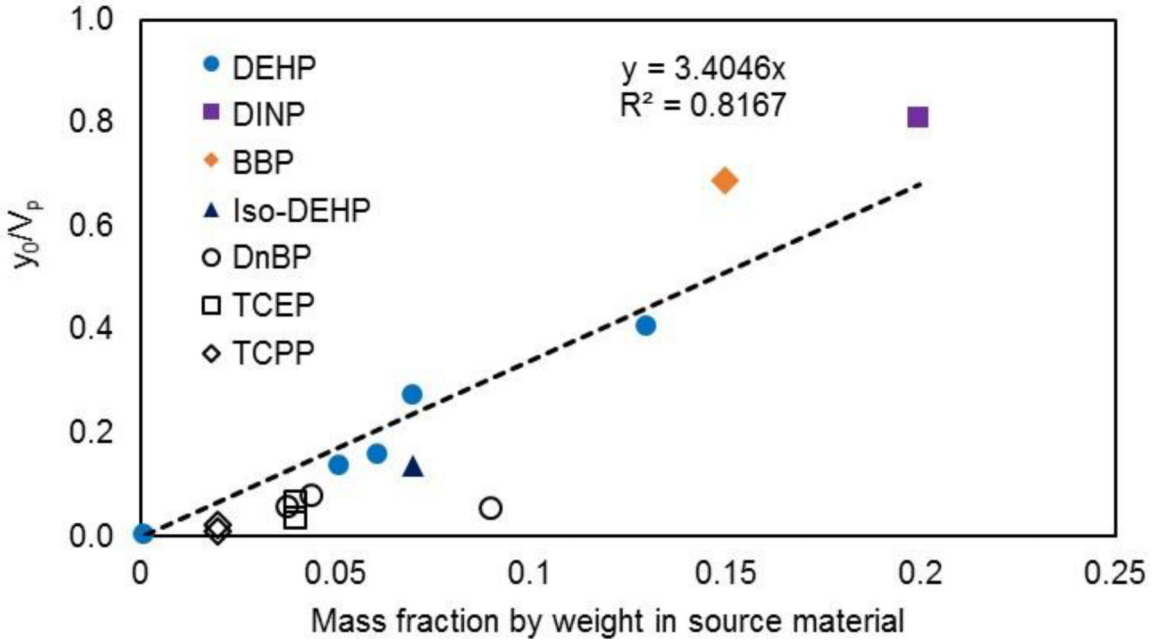

Figure 2.

Relationship between y_0/V_p and compound mass fraction in material for SVOCs at room temperature.

Table 1.

Parameters Obtained from the M-A-M Microchamber Emission Test, the Diffusive Sampling Test, and the Dual Small Chamber Sorption Test

tests	parameters		TCEP	TCPP	TDCPP
microchamber emission test[a]	y_0 (Test 1)	$\mu g/m^3$	8.75	3.64	N/A
	y_0 (Test 2)	$\mu g/m^3$	8.11	3.64	N/A
	average y_0	$\mu g/m^3$	8.43	3.64	N/A
diffusive sampling test[b]	y_0 (Position 1)	$\mu g/m^3$	4.10	1.60	4.30
	K_{sa} (Position 1)	m	160	350	550
	y_0 (Position 2)	$\mu g/m^3$	4.50	1.70	4.40
	K_{sa} (Position 2)	m	140	340	620
	y_0 (Position 3)	$\mu g/m^3$	4.40	1.70	4.50
	K_{sa} (Position 3)	m	140	325	560
	average y_0	$\mu g/m^3$	4.33	1.67	4.40
	average K_{sa}	m	146.67	338.33	576.67
dual small chamber sorption test[c]	D_m	m^2/h	2.01×10^{-10}	8.25×10^{-11}	1.39×10^{-11}
	K_{ma}		7.76×10^6	6.85×10^6	1.90×10^8
	y_0[d]	$\mu g/m^3$	116.47	77.85	16.26

[a] Calculated by eq 5.

[b] Obtained from model fitting following the method described in ref 29.

[c] Obtained from model fitting following the DSS model

[d] Calculated by eq 7